ANNUAL REVIEWS

Annual Review of Control, Robotics, and Autonomous Systems

Stretchable Shape Sensing and Computation for General Shape-Changing Robots

Stephanie J. Woodman and Rebecca Kramer-Bottiglio

Department of Mechanical Engineering, Yale University, New Haven, Connecticut, USA;
email: rebecca.kramer@yale.edu

ANNUAL REVIEWS CONNECT

www.annualreviews.org

- Download figures
- Navigate cited references
- Keyword search
- Explore related articles
- Share via email or social media

Keywords

shape sensing, soft robotics, stretchable electronics, stretchable computation, morphing robots

Abstract

An ideal robot could autonomously complete diverse tasks such as ocean surveying, kitchen cleaning, and aerial environmental monitoring. However, robots optimized for each task typically have different shapes, posing a challenge in reconciling form and function. This challenge inspires the pursuit of general shape-changing robots (GSCRs). While soft materials and actuators are promising for GSCRs due to their ability to accommodate extreme deformations, there is a gap between the vision of GSCRs and the simple examples we see today. Two critical components are needed: robot-agnostic stretchable shape sensing and stretchable computing. Together, these components would enable closed-loop shape control and the first instantiations of GSCRs. This review aims to consolidate the literature on these components, encouraging researchers to bridge the gap between today's shape-changing robots and the envisioned GSCRs, ultimately advancing the field toward more versatile and adaptive robots.

1. INTRODUCTION

General shape-changing robots (GSCRs) have incredible potential to fulfill the original vision of robotics: machines that can do anything. From aerial to quadruped to aquatic body types, GSCRs could explore any environment and perform myriad tasks with just one set of finite hardware (**Figure 1**). Initial versions of morphing platforms have been attempted in many ways, from a single system with constant material (rigid, soft, or hybrid) that changes shape (1) to reconfigurable robots that can add and subtract body material (2, 3), though the latter are outside the scope of this review. Techniques from the field of soft robotics are uniquely promising for shape-changing systems since, fundamentally, a change in shape necessitates surface strains (4) that are accommodated by the base materials in soft robots (5–7), which can stretch up to 1,000% (8). However, we have yet to see a platform capable of generalized shape change. Why is this, and how do we get there? This review aims to answer these questions and give members of the field a concrete path to creating GSCRs with closed-loop control over their shape.

First, what is a shape-changing robot, what is a GSCR, and what is neither? In a previous review, Shah et al. (1) used the term shape-changing robot to refer to "robots that actively change their shape to adapt to their environment or gain new functionalities" (p. 2). A later work (9) augmented this definition to further specify a shape-changing robot as a robot that can change its resting (unactuated) shape to adapt to new environments or gain functionalities. The latter definition does not necessarily mean that all actuators employed for shape change must be at rest in the new shape; rather, it indicates that the actuators used to hold a new shape are not also used for gait actuation while in that shape. For example, the three-banded armadillo is typically a legged quadruped but can tuck its head, legs, and tail into its shell and roll to escape predation. A robot that mimics such coupled shape and gait adaptation would meet our definition of shape changing. It is not our intent to divide robots into exclusive categories, but rather to provide a framework to discuss the state of shape-changing robots and highlight the technology advances that may push the field toward our vision of GSCRs.

A GSCR represents an extreme instantiation of a shape-changing robot (**Figure 1**). The robots of this vision can freely change between arbitrary and nearly unlimited shapes as needed and have onboard proprioception, sensing, and control. Exhibiting adaptive morphogenesis (10), they
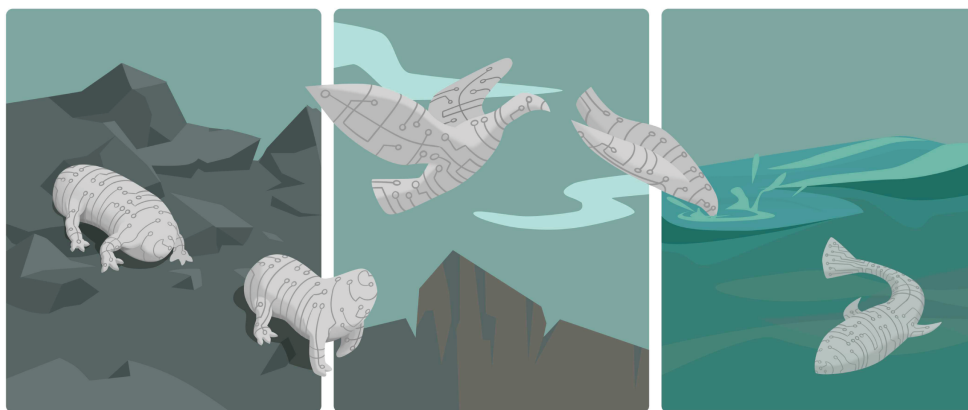
Figure 1

Illustration of the vision of general shape-changing robots. These robots will know their own shape, have onboard control over their shape, and be able to morph into nearly any shape on demand. Illustration created by Fernanda Nevitiv da Costa.

can adapt to changing environments and task demands to efficiently accomplish their objectives. Though this vision has only been seen in science fiction, we hope to convince the reader that the field is only a few key innovations away from its first instantiations.

With these definitions and vision, we examine examples and non-examples of current shape-changing systems. Then, we highlight what can be learned and identify sensing- and computation-specific gaps in the current approaches, which when filled may enable the realization of GSCRs.

## 1.1. What Robots Are Not Shape-Changing Systems?

So, what robots are not shape-changing systems? Though the robot Tetraflex from Wharton et al. (11) is an impressive platform that looks like it is constantly changing shape by altering the lengths of its sides to offset its center of gravity, this does not meet our definition of shape changing, as the apparent changes in shape are used primarily to execute a gait. A second example of this consists of an inflatable sphere with sections along its surface that can jam using granular jamming (12). The jammed sections on the surface, in this case, control the shape by directing how the single actuator can expand the shape, and the robot uses this shape change to roll. Though this is a locomoting robot that changes shape, it, like Tetraflex, uses the shape change only to locomote.

Many gait-changing robots exist and are able to gain access to varying environments using new gaits (5, 13, 14), but just changing gait does not meet our stricter definition of a shape-changing robot and work toward the vision of GSCRs. Though a humanoid robot could, in theory, swim, walk, and dig, it would accomplish these tasks inefficiently, wasting precious onboard power and time, and still never be able to fly, squeeze through small gaps, or adapt its limbs to manifest the tools needed to accomplish a task on the spot. GSCRs would be able to accomplish all of these tasks efficiently by changing shape. Additionally, pose-changing robots, like most continuum arms (15, 16), do not fall under our definition. For example, McEvoy & Correll (15) and Stella et al. (16) were able to change the pose of a continuum manipulator, but we see this as actuation of the robot.

An adjacent field to shape-changing robots is that of shape-morphing surfaces. In this field, vital material and actuation developments have been made to create surfaces that change shape (17–23), but they are generally not robots—they use their actuators only to change shape and exhibit no other function or new ability. However, the techniques from this field are and will be useful for the field of shape-changing robots, as their methods of high-degree-of-freedom (high-DOF) actuation will aid designers of future shape-changing robots. For example, Zhang et al. (22) used variable-stiffness shape-morphing hydrogels to achieve multiple shapes in 3D.

1.2. What Shape-Changing Robots Exist Today?

What are some current examples that meet our definition of a shape-changing robot? The previous work that first introduced the term resting shape (9) put forward a soft robot that exemplifies our definition: The robot has an internal bladder that can be inflated or deflated and several surface actuators to execute gait (**Figure 2a**). Depending on the inflation of the internal bladder, the robot is in one of two resting shapes, flat or cylindrical, and the actuators are used to inch the robot or roll it, respectively, to operate on flat ground or an incline. Another prior work (27) used robotic skins to mold a lump of clay, changing the resting shape of the robot to avoid obstacles and then other actuators to execute a gait. Another early example by Lin et al. (24) demonstrated an inchworm-inspired robot that can morph into a circular rolling robot to increase movement speed (**Figure 2b**).
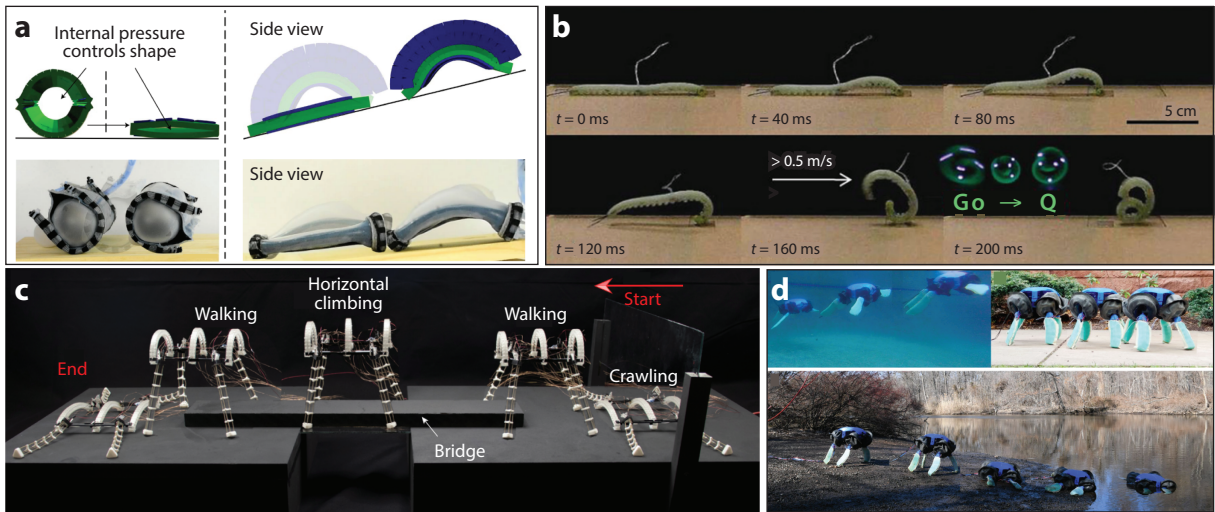
Figure 2

Today's soft and hybrid shape-changing robots. (*a*) A soft robot that uses an internal bladder to change its shape and locomote in different environments. (*Left*) The inner bladder expanding in simulation and expanded in real hardware. (*Right*) The robot inching up an incline with a deflated internal bladder. Panel adapted from Reference 9. (*b*) A soft robot that goes from an inching to rolling gait using shape change. (*Top*) The robot inching. (*Bottom*) The robot using a ballistic rolling gait. Panel adapted with permission from Reference 24. (*c*) A hybrid rigid–soft robot that switches between a low-profile crawling gait and a walking gait to traverse different environments. This example achieves closed-loop control over its shape. Panel adapted from Reference 25 (CC BY 4.0). (*d*) A hybrid rigid–soft robot that can morph its limb shape to swim in water (*top left*), walk on land (*top right*), and transition between environments (*bottom*). Panel adapted from Reference 26.

Several rigid–soft hybrid robots are able to adjust the height or curvature of parts of their bodies to access new environments (26, 28), where their gait is separate from the shape change. Another entirely rigid robot walks with the same gait while controlling the length of its legs (29), using this shape change to move efficiently in different terrains. A soft tensegrity robot uses extendable rods to access other gaits—for example, it extends a strut to change its shape, then rapidly extends two other struts to stably roll (30). A few notable examples demonstrate shape-changing abilities to access different modes of transport by curving the centers of their bodies. One example transitions from a shape favoring crawling to one that supports walking (25) (**Figure 2c**). Other examples morph from a terrestrial locomotor to a flying robot (31, 32). Like the above, many of today's shape-changing robots have only one part of the robot change shape. For example, the wheel of the robot can change its size (33, 34), or a flipper can morph into a leg to access aquatic and terrestrial environments (26, 35) (**Figure 2d**). Though these are state-of-the-art examples, they generally execute a low-DOF shape change.

To further analyze these examples, **Table 1** compiles some key metrics on shape-changing systems. From this table, we glean that the average numbers of degrees of freedom for shape-changing robots classified as soft, rigid, and hybrid are 8.8, 4.5, and 1.8, respectively. Rigid robots have fewer DOFs than soft robots (but generally the same order of magnitude). However, it is difficult to imagine much higher-DOF shape change in rigid systems, as they would need an increasingly complex and clunky actuation scheme due to the addition of many motors, linear actuators, and so on. Hybrid examples present an interesting compromise between soft morphing and the controllability of rigid robots, leading to highly functional robots but the most limited number of attainable shapes (25, 26).

Table 1   Today's shape-changing robotic systems

Reference	Soft, rigid, or hybrid?[a]	DOFs for SC[b]	Open-loop control[c]	Closed-loop control[d]
Hwang et al. (31)[e]	Hybrid	1	Shape and gait[f]	NA
Shah et al. (9)	Soft	1	Shape	Gait
Lee et al. (33)	Hybrid	1	Shape and gait[g]	NA
Wilcox et al. (32)	Rigid	1	Shape and gait	NA
Lin et al. (24)	Soft	2	Shape and gait	NA
Sun et al. (25)	Hybrid	3–4[h]	Gait	Shape
Baines et al. (26)	Hybrid	4	Shape and gait	NA
Nygaard et al. (29)	Rigid	8	NA	Shape and gait
Jeong et al. (30)[i]	Soft	12	Shape and gait	NA
Shah et al. (27)	Soft	20	Shape and gait	NA

Abbreviations: DOF, degree of freedom; NA, not applicable; SC, shape change.

[a]A system is denoted as soft if a load can be applied in any direction and the system exhibits bulk compliance, rigid if it is composed entirely of regions that are incompressible, and hybrid if it has components traditionally used in soft robotics that exhibit the above compliance, but a portion of the robot is incompressible.

[b]The number of DOFs possible in the system with the actuation scheme. For example, in Reference 25, the crawler/walker uses three actuators to change the body shape; because the three actuators always actuate together, there is only one DOF in their demonstration, but three potential DOFs for shape change in the system. The same applies to Reference 26: Four flippers can change their shape, though the robot only achieves two distinct shapes by using all four simultaneously.

[c]A system is denoted as exhibiting open-loop control if it has no sensor giving high-level feedback or is controlled remotely by human input (e.g., a human driving a system with wheels or rotors).

[d]A system is denoted as exhibiting closed-loop control if it has a sensor whose feedback enables autonomous high-level gait/trajectory or shape change autonomously with no human in the loop.

[e]Land and air transport machine.

[f]Driven and flown using remote control.

[g]User controlled.

[h]Three for the crawler/walker, and four for the quadruped with four legs.

[i]The type 3 jumping robot in the paper.

1.3. What Is Preventing the Transition from Today's Shape-Changing Robots to General Shape-Changing Robots?

All of today's examples are limited in the number and diversity of shapes they can achieve, with soft systems achieving DOFs larger than, but often on the same order of magnitude as, their hybrid and rigid counterparts. Soft robots' higher DOFs indicate their promise for GSCRs, so why has no one in soft robotics ventured to create a system with much higher DOFs, especially when such diverse soft actuation techniques have been presented? The answer to this question could be due to another fact that can be drawn from **Table 1**: No soft shape-changing robots have achieved closed-loop control over shape.

Though some shape-changing robots have achieved closed-loop control of their gait or reliable open-loop gaits (26), these demonstrations were achieved largely with easily sensed and controlled rigid motors (as used in hybrid and rigid robots) (25, 29), so the state of the robot was known. No fully soft robot had the sensing technology needed to achieve closed-loop control of its shape. One hybrid robot used the self-sensing property of its soft actuator (25), which, when calibrated with the control signal, could indicate the curvature of the body and, hence, the state and shape of the robot. For the simple, low-DOF systems in **Table 1**, traditional sensing can and has worked to close the loop on shape, but for GSCRs, current sensing technology fundamentally will not work.

Current soft sensing technology compatible with soft robot bodies works by measuring deviations from a zero-strain state and applying material-dependent models to estimate the

deformations within the confines of the model (36–41). Suppose a continuum arm has a stretchable strain sensor embedded in it, and the cylinder deforms to the right. In that case, the soft cylinder can be reconstructed after having deviated from the initial, resting model of the cylinder. However, for GSCRs (**Figure 1**), the resting shape/zero-strain state is constantly being deformed and updated. Such complex actuation schemes would be incredibly difficult, if not impossible, to model (42, 43), and even if it were possible, the robot model and performance would change when covered in the large number of strain sensors needed to enable generalized deformation. If it could indeed accommodate so many sensors, the compound error from the sensors during these large deformations would yield nearly unusable results. Hence, current soft sensing technology fails in the case of GSCRs.

Thus, achieving proprioception and, subsequently, closed-loop shape change in GSCRs requires robot-agnostic, onboard shape sensing capable of withstanding the strains necessary for the drastic, high-DOF shape changes afforded by soft robots. This lack of sensing is the first and primary reason that GSCRs have not advanced: The robot needs to reliably know its shape and state, no matter how complex the deformation, and use this information to change shape and control a new gait on demand. However, to integrate this high deformation sensing into the surfaces of these robots and effectively control the robot in any given shape, environment, or task, we need to embed state-of-the-art electronics that can also withstand these strains. These electronics will connect the sensors across the surface, perform local and global sensor processing, and execute control policies—eventually executing onboard, untethered closed-loop control of shape, gait, and task. To achieve this, in addition to robot-agnostic stretchable shape sensing, we also need robust, highly stretchable computing platforms that can perform as well as today's rigid electronics and be embedded into the surfaces and bodies of shape-changing soft robots without inhibiting stretch.

These are the two major gaps between the soft shape-changing robots of today and GSCRs: robot-agnostic stretchable shape sensing and embedded soft electronics for computation. This review covers the state of the art in (*a*) embodied, robot-agnostic sensing approaches that can accommodate strain and (*b*) highly stretchable circuits with state-of-the-art computing in soft robots, and then summarizes major next steps for the field to achieve the GSCRs illustrated in **Figure 1**.

2. ROBOT-AGNOSTIC SHAPE SENSING FOR GENERAL SHAPE-CHANGING ROBOTS

Like robots, many sensing platforms use the term shape when they really capture a change in pose or posture (e.g., of a continuum arm) by leveraging an initial mechanical model of the system. These sensing techniques are invalid for GSCRs due to their dependence on a model of the robot to reconstruct shape from their raw sensor data. As outlined above, because of the generalized shape-changing ability of GSCRs, their sensing technology cannot depend on a model of the hardware of the robot—they must be robot agnostic.

To date, only a small effort has been made to achieve stretchable, robot-agnostic shape sensing for soft robots. In this section, we review (*a*) current proprioceptive techniques for soft robots that depend on models of the robot hardware (learned or analytical) to reconstruct robot pose and (*b*) the efforts toward robot-agnostic shape sensing across fields—the combination of which, we believe, will ultimately become standard on shape-changing soft robots.

2.1. Traditional, Robot-Dependent Shape Sensing and Proprioception

Soft robots use a variety of sensing technologies to estimate their shape and state. A pervasive form of soft sensing is stretchable strain sensing. This can be accomplished using either capacitive

(37, 38, 44) or resistive (36, 45, 46) techniques, often withstanding large strains (>300%) (37). Another common technique that measures bending, stretching, and even temperature is optical sensing, including fiber optics (41, 47, 48), fiber Bragg gratings (49), and optoelectronic sensory foams (50). It is also efficient to use actuators as the sensors, for example, using twisted and coiled actuators (25) or shape memory alloy actuators (51). Many of these sensing techniques pair the sensor data with machine learning to estimate the pose of their robot (39, 40, 47, 50).

The robot model-dependent techniques reviewed above exhibit excellent robustness to strain and can be easily embedded in the bodies of today's soft robots (52). However, they are limited to capturing simple deformations due to challenges in modeling and sensor placement/complexity in soft robotic systems (42, 43). To overcome this limitation and extend beyond sensing only what can be modeled, we need robot-agnostic shape sensing that can withstand the same strains as traditional soft sensors.
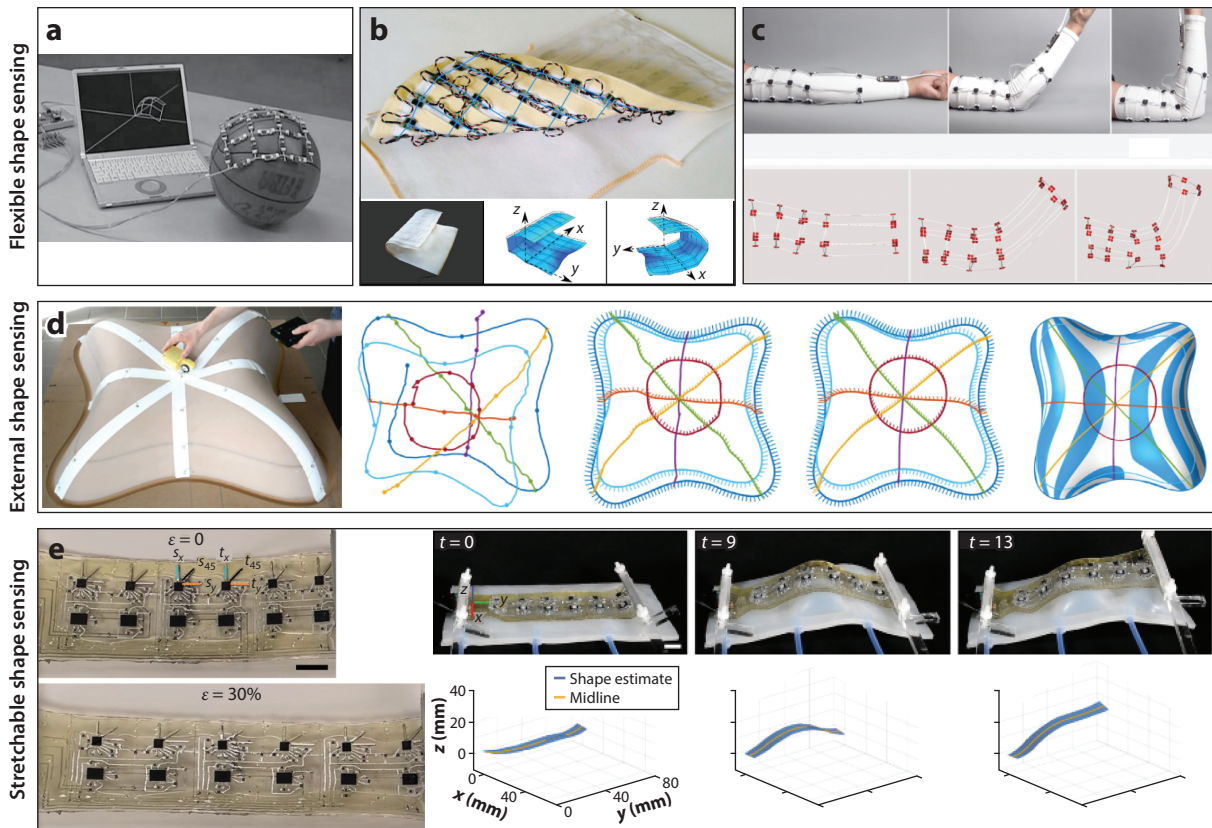
2.2. Stretchable, Robot-Agnostic Shape Sensing

Work on surface-based, robot-agnostic shape sensing has been ongoing for some time in the world of computer graphics, for use during instances when occlusions make shape or object reconstruction difficult. For example, Hoshi & Shinoda (53) introduced a simple grid of inertial measurement unit (IMU) arrays fixed together by rigid links that could bend around objects to detect shape by reconstructing a grid (**Figure 3a**). Work by Saguin-Sprynski and colleagues (58–61) has developed shape reconstruction algorithms based on differential geometry, from flexible ribbons to sheets of IMUs, yielding smooth reconstructions of shape. Hermanis et al. (54) also embedded IMUs into fabric and approximated shape using a rigid link approximation (**Figure 3b**). Similarly, Zhou et al. (55) built custom flexible printed circuit board (PCB) arrays with nodes of IMUs dependent on the application (**Figure 3c**), and Hu et al. (62) used arrays of IMUs to approximate the 2D cross section of 3D objects. In addition to IMU arrays, piezoelectric sensors have been patterned into flexible sheets, using machine learning to enable self-sensing (63). These sheets can then be applied to various structures to approximate their shape.

The solutions described above allow the sensing platform to be placed on any robot to continuously estimate its shape, even as it changes. However, these solutions are only flexible and cannot accommodate the stretch required for GSCRs. The need for stretchability, or at least for a less physically constrained system, has been addressed without stretchable technology by using patches and an external vision system to estimate shape (64), and even by using a small hand cart that can roll along surfaces to collect orientations and distances along the surface (56) (**Figure 3d**). From systems utilizing external mechanisms, we have learned that with orientations on a surface and the distances between them, any shape can be reconstructed, even under strain. The key is to incorporate distance sensing into an onboard platform.

The first effort to combine soft robotic techniques with previous inextensible, robot-agnostic shape-sensing methods involved using stretchable electronics. This approach embedded IMUs in a stretchable sheet integrated with liquid metal–based strain sensors (57) (**Figure 3e**). Stretching up to 30%, this ribbon of sensors estimated the 2D shape of static and dynamically stretching objects. This work was then built upon by making a version more robust to consistent stretching, using stretchable sensors and rigid PCBs, and 2D shapes were approximated under varying strains of the system (up to 40%), showing only minor increases in mean absolute error (65).

Methods beyond combining stretch sensors and IMUs show promise as well, such as integrating a self-sensing fiber Bragg grating (66) into an elastomer substrate, though this approach suffers from lower stretchability (∼<5%). Another group introduced an inductance sensor array that could estimate surfaces but would be difficult to miniaturize and embed in a unified robotic

Figure 3

Robot-agnostic shape sensing. (*a*) A flexible array of IMUs and microcomputers. Image reproduced with permission from Reference 53; copyright 2008 SICE. (*b*) A flexible fabric sheet for shape reconstruction, showing the sheet hardware (*top*) and the reconstruction (*bottom*). Images reproduced with permission from Reference 54. (*c*) A customized grid of IMUs for wearable shape sensing, showing the real motions (*top*) and the reconstruction (*bottom*). Images reproduced with permission from Reference 55. (*d*) Algorithm to use distances and orientations along a surface to reconstruct shape using an external sensing system, showing the data collection scheme (*left*) and the reconstruction process (*right*). Images reproduced with permission from Reference 56. (*e*) A stretchable ribbon of orientation and stretch sensors to reconstruct shape, showing the stretch (*left*) and the reconstruction (*right*). Panel adapted from Reference 57 (CC BY 4.0). Abbreviation: IMU, inertial measurement unit.

system (67). We also note an interesting technique in which a rigid robot arm used an algorithm to determine its topology by randomly actuating and gleaning which joints were neighbors from crosstalk (68), a principle that could potentially be applied to soft actuator types in the future.

These robot-agnostic shape-sensing methods are summarized in **Table 2**. From this table, we glean several key takeaways:

- Current robot-agnostic shape-sensing methods are largely surface based, requiring sensors and electronics along the surface of the shape or body.
- Early robot-agnostic shape-sensing techniques do not allow stretch or surface strains.
- Common techniques use orientation sensors spaced along the surface with known or measured distances between them to reconstruct shape.
- Many robot-agnostic shape-sensing methods are incompatible with high-strain, soft robotic systems.

Table 2   Robot-agnostic shape-sensing techniques

Reference	Approach[a]	Shape reconstruction technique[b]	Shape dim.[c]	Sensor location[d]	Max. stretch.[e]	Resolution[f]
Hoshi & Shinoda (53)	Flexible array of IMUs	Rigid link	3D	Surface	NA	5.5 cm
Sprynski et al. (58)	Flexible PCB ribbon of IMUs	Differential geometry	3D	Surface	NA	3 cm
Huard et al. (59)	Flexible PCB ribbon of IMUs[g]	Differential geometry	3D	Surface	NA	3 cm
Huard et al. (60)	Flexible PCB ribbon of IMUs	Differential geometry	3D	Surface	NA	3 cm
Saguin-Sprynski et al. (61)	Array of IMUs on textile	Differential geometry	3D	Surface	NA	12.5 cm
Mittendorfer et al. (64)	Camera and markers	Marker position reconstruction	3D	Offboard	NA	~2.4 cm
Rendl et al. (63)	Piezoelectric sensors on flexible film	Self-sensing using machine learning	3D	Surface	NA	NA
Hermanis et al. (54)	Array of IMUs on textile	Rigid link	3D	Surface	NA	3.5 cm
Stanko et al. (56)	Wheeled cart with IMU and encoders	Differential geometry	3D	Offboard	NA	NA
Zhou et al. (55)	Flexible array of IMUs	Radial basis function interpolation	3D	Surface	NA	Variable
Hu et al. (62)	Ribbon of IMUs	Differential geometry	2D	Surface	NA	20 cm
Lun et al. (66)	Fiber Bragg grating in silicone	Self-sensing using machine learning	3D	Surface	< 5%[h]	NA
Shah et al. (57)	Stretchable electronic circuit with IMUs and stretch sensors	Rigid link and differential geometry	2D	Surface	30%	1.7 cm
Woodman et al. (65)	Ribbon of IMUs and textile stretch sensors	Differential geometry	2D	Surface	40%	7 cm
Soleimani et al. (67)	Mutual inductance sensor array	Self-sensing using inversion, calibration, and machine learning	2D	Surface	~50%[i]	NA

Abbreviations: IMU, inertial measurement unit; NA, not applicable; PCB, printed circuit board.

[a]Implemented sensing hardware or principle.

[b]How the sensor data were processed to reconstruct the shape; some techniques connect nodes along the surface using rigid links, while others use methods in differential geometry to achieve smooth results.

[c]Reconstructed shape dimension, specifying whether 2D or 3D shapes were reconstructed.

[d]Where the sensing hardware was positioned relative to the robot.

[e]Maximum stretchability (maximum percent strain) reported.

[f]Resolution or distance between nodes in a sensing array; for stretchable systems, this distance is measured at rest.

[g]The ribbon is placed in multiple positions on a 3D surface.

[h]The elastomer stretches minimally with the embedded sheet, although it is not quantified in this work.

[i]For 1D shape sensing.

- ■ The average resolution of sheet- or ribbon-based sensing techniques is 6.16 cm, with the minimum being 1.7 cm (57).

It is clear that we have yet to truly achieve integrated, robot-agnostic, 3D shape sensing capable of withstanding the strains of future GSCRs, though a few works that utilize IMUs and stretch sensors together are getting close.

The next work in this space should focus on (*a*) increasing the stretchability of current methods (e.g., by removing rigid structures that would inhibit shape morphing), (*b*) increasing the level of integration of shape-sensing materials and hardware into the surfaces of soft robots, and (*c*) increasing the resolution of sensing arrays to capture more detailed shapes. One notable work indeed tackled stretchability, integration, and resolution (57) by using techniques in stretchable electronics to create a much softer, tightly integrated sensing array. In this design, the only rigid components were the integrated circuits (ICs).

As indicated experimentally (65) and theoretically (69), at least two orientations per curve on the surface are required to reconstruct a shape accurately. For detailed and small-scale shapes, the sensor hardware must necessarily also be smaller and more tightly spaced to recreate the shape. For stretchable IMU arrays, this means minimizing IMU node size and spacing and making the rigid components as small as possible to allow stretch. In addition, while we expect actuator expansion to execute shape changes, there will also be necessary shrinkage of actuators. Therefore, sensing platforms should both accommodate and capture shrinkage.

To propel the field of robot-agnostic stretchable shape sensing forward, we will need circuitry capable of connecting these sensors across the surfaces of soft robots, processing sensor data, and executing control policies and commands, all without inhibiting the high-strain shape change of GSCRs. Thus, advancements in stretchable electronics that can be embedded into the bodies of high-strain soft robots and exhibit state-of-the-art computational power are essential to enabling GSCRs.

3. STRETCHABLE COMPUTATION FOR GENERAL SHAPE-CHANGING ROBOTS

Highly stretchable electronics with state-of-the-art computational power and component density have remained an open challenge in soft robotics. However, overcoming this challenge will be pivotal for the advancement of GSCRs. Without solutions, soft roboticists have moved electronics and actuators offboard (70) or compromised with rigid sections of their soft robots (71). However, there have been efforts toward stretchable computation suitable for embedding into soft robots. Two main categories of stretchable computation exist: those comprising entirely soft logic—for example, using pneumatics (72–75), microfluidics (76, 77), or other material properties (78)—and those converting rigid PCBs into soft and stretchable versions while maintaining rigid ICs and passive components (79, 80). This review focuses on the latter category, as it maintains state-of-the-art computational ability relative to soft logic gates.

Many strategies have been put forward to create PCBs with stretchable substrates and conductors (81), such as liquid metal–based traces (82), copper traces that have been geometrically patterned to allow stretch (79, 83, 84), and conductive composites (85). Circuits with liquid metal–based traces generally exhibit high conductivity and are theoretically limited in stretchability only by the material encasing them. These factors make liquid metal–based conductors excellent candidates for the high-strain circuits required for GSCRs.

The most prevalent liquid metal used for stretchable electronics is a eutectic gallium-indium alloy. This material has been modified in many ways to be used for stretchable electronics (86, 87), including formulation modifications affecting the rheological properties (88), electromechanical behavior (89–92), and conductivity (93). However, we have yet to see liquid metal–based complex circuits integrated into high-strain robotic systems.

While many authors showcase circuits as a demonstration of their process or material, these circuits are often applied to systems in locations experiencing low or no strain (94–96). For example, a stretchable circuit placed adjacent to, but not directly over, a joint in a wearable demonstration

will experience relatively low strains compared with the strains expected in GSCRs. Additionally, the strain-dependent performance of so-called stretchable circuits is often not characterized (97–99), with a few counterexamples (82, 89, 100–103) (**Figure 4a**). We posit that such strategic placement and/or lacking characterizations are largely due to challenges in interfacing rigid microelectronic components with soft traces, soft traces with substrates and encapsulants, and combinations thereof. Stress concentrations between rigid and soft materials lead to breakage, or bridging of conductive traces. Imperfect bonding between encapsulating and substrate materials, or between substrate materials and IC packaging, can also lead to failure modes. In sum, stretchable circuits face challenges at material interfaces, which likely compels designers to reduce the complexity of their circuits, the amount of strain applied to them, or both.

In this section, our aim is to review the literature on stretchable computation, focusing on the quality of the most complex circuits presented in each paper. We seek to describe how this field must evolve to meet the demands of GSCRs and realize integrated stretchable computation in soft robots. We begin with **Table 3**, which compiles recent works on stretchable computing that are within the bounds of our aforementioned focus. This table also introduces the concept of a complexity number—the number of rigid–soft interconnects divided by the number of microelectronic components. If a paper had multiple circuits, the one with the highest complexity number was chosen and evaluated in the table. **Figure 5** plots the amount the circuit stretched against the complexity number for each paper.

From **Table 3**, we glean several key takeaways:

- Many researchers have successfully integrated ICs into circuits with resolutions on the order of 200 μm using various manufacturing techniques and substrates.
- The maximum strain of the most complex circuit (in a given work) is not often reported. Complex circuits are often treated as demonstrations, lacking comprehensive characterization.
- Most demonstrations of complex circuits are in low-strain/no-strain applications.
- Of the 21 works included in **Table 3**, nine have a complexity number of at least 3 (82, 94, 97, 98, 100–102, 109, 110).
- The highest strain withstood by a complex circuit was 404% (102).
- Four works in **Table 3** embedded their circuits in soft robots (97, 101, 102, 109).

Figure 5 also provides several key findings:

- Complexity numbers greater than 2 indicate that there was at least one component in the circuit that was not a simple resistor, LED, capacitor, diode, etc.
- More complex circuits with complexity numbers of at least 3 are rarely strained more than a few percent during bending and are rarely characterized.
- While a couple of circuits were strained to between 300% and 400% in isolation (101, 102), when integrated into soft robots, they experienced strains of approximately 100% (102).

To illustrate the utility and usage of the complexity number, we explicitly mention a few special cases and examples. Several of the referenced works use only passive microelectronic components, like LEDs (91, 103, 105), so although they have a large number of components and interfaces, their complexity number is 2. Works with higher complexity numbers have at least one IC component with multiple connections, indicating more state-of-the-art design and computational capability. One example of note is the paper by Huang et al. (84), who used geometric patterning of copper traces to create a four-layer circuit, but since there were no rigid–soft interfaces, it has a complexity number of 0.
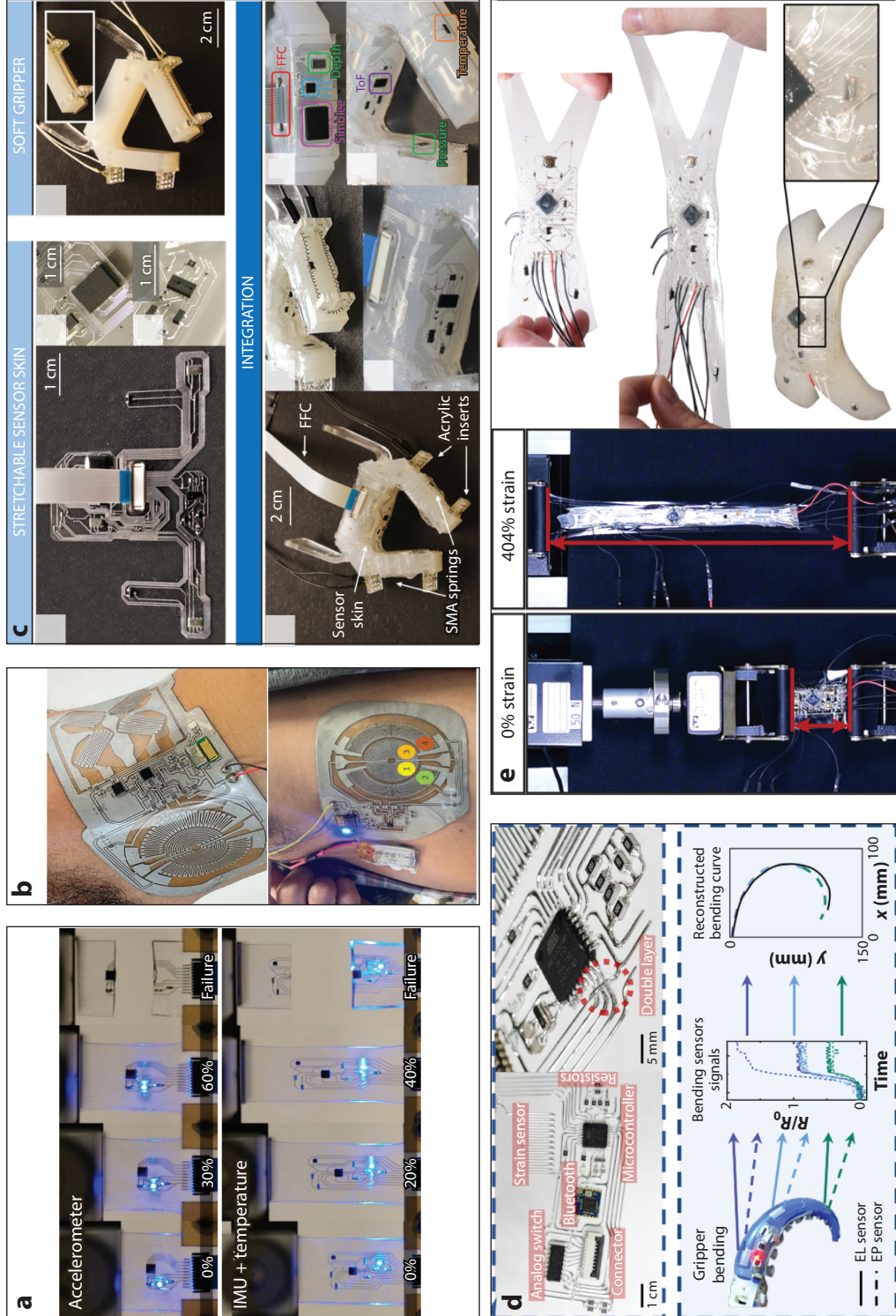
(Caption appears on following page)

Figure 4 (*Figure appears on preceding page*)

Stretchable and embedded electronics for onboard computing. (*a*) Two PDMS-based stretchable electronic circuits being strained to failure using a mechanical testing device [an accelerometer (*top*) or an IMU and temperature circuit (*bottom*)]. Panel adapted with permission from Reference 100. (*b*) Wearable demonstrations of stretchable circuits with integrated computation and sensing. Images reproduced with permission from Reference 104. (*c*) A stretchable circuit embedded in a soft robotic gripper. The circuit is shown (*top left*), along with the gripper (*top right*) and the integration of the two (*bottom*). Panel adapted with permission from Reference 97. (*d*) A stretchable circuit with computational processing, Bluetooth, and sensing integrated into an octopus tentacle, showing the circuit before integration (*top*) and integrated into the gripper (*bottom*). Panel adapted from Reference 101 with permission from AAAS. (*e*) A stretchable Arduino Pro Mini being tested using a mechanical testing device at low and high strains (*left*) and embedded into the stretching portion of a soft robot (*right*). Panel adapted with permission from Reference 102. Abbreviations: EL, elongation; EP, expansion; FFC, flat flexible cable; IMU, inertial measurement unit; PDMS, polydimethylsiloxane; SMA, shape memory alloy; ToF, time-of-flight range chip.

In conjunction with the complexity number, the number of layers in a circuit is important for achieving high computational capacity in a small space. Most commercial PCBs today are two or more circuit layers, which helps minimize board size and cost. Notably, nine of the 21 papers tabulated are only one layer (82, 94–97, 100, 108–110), while nine are two layers (89, 91, 98, 101–104, 106, 107), and two are more than two layers (84, 105). Hence, a significant number of works meet the standard two-layer designs of rigid PCBs today, but there is still work to do to develop the manufacturing procedures to adapt to double- and multilayer circuits.

While many of these works demonstrate complex circuits, few provide a full characterization of the entire circuit; instead, they typically characterize only a single trace under strain. Even fewer characterize multiple samples of their circuits under strain. This presumably stems from challenges in interfacing between rigid and soft components, since some traces strain up to 900% alone (94), while the complete complex circuits are not strained. A notable and consistent commonality among many papers is that the complex circuit is utilized as a wearable in demonstration. Though these demonstration circuits show utility, even making complex temperature/humidity (94), electrocardiogram (110), and optical/thermal (104) sensor circuits (**Figure 4*b***), they often do not show or characterize strain, though some show bending (96) or a few percent strain in supplemental videos (95). Ultimately, there are only a few examples of circuits embedded into soft robot bodies (**Figure 4*c,d***), and just one showing functionality during high-strain use of the soft robot (102) (**Figure 4*e***).

The lack of characterization and high-strain demonstrations potentially points to a central challenge in the field of stretchable computing that needs to be traversed in order to enable soft computation for high-deformation, soft GSCRs with state-of-the-art-compute: interfacing. Interfaces between ICs and soft conductors, soft conductors and substrates, substrates and encapsulants, ICs and substrates, and ICs and encapsulants are often failure points in stretchable circuits. Solutions to challenges in interfacing could be addressed at the material level, by introducing strain gradients into the substrate to mitigate stress concentrations around rigid components, for example, by adding stiffer materials around stiff components (101, 102). Stiff materials could also be integrated directly into the substrate (i.e., through substrates designed with stiffer portions under rigid components) to mitigate stress concentrations more effectively. The same concept could be applied to the soft conductor: It bonds well with and is rigid at the point where it contacts the rigid component but softens into a liquid as it grows farther from the substrate, allowing stretch. Additionally, solutions in adhesion and bonding between substrates could mitigate these issues. If bonding were perfect between the packaging of an IC component and the soft substrate, then trace bridging between pins would be much less likely. In a similar vein, perfect bonding between the substrate and encapsulant would prevent soft trace materials from bridging to other traces.

In addressing the above challenges, the field will naturally migrate from work on stretchable conductors with circuits as demonstrations to full characterization of stretchable computation

Table 3 Performance of stretchable electronic circuits

Reference	ICs?	Trace manufacturing technique	Num. layers[a]	Min. TW (μm)[b]	Max. strain (%)	Substrate	Application	Strain during application (%)	Num. rigid–soft interf.[c]	Num. rigid comp.[d]	Complexity num.[e]
Huang et al. (84)	Yes	Geometric patterning	4	150	50	PDMS	Wearable	ND	0	56	0
Chen et al. (91)	No	Stencil printing	2	200	ND	TPU or VHB	Wearable	ND	40	20	2
Song et al. (105)	No	Photothermal patterning	3	250	30	PDMS	Wearable	ND	50	25	2
Lee et al. (103)	No	Omnidirectional 3DP	2	100	40	PDMS	Wearable	ND	30	15	2
Lee et al. (106)	Yes	Stencil printing	2	200*	ND	VHB	NA	ND	24	11	2.18
Li et al. (107)	Yes	Solid wire fabrication	2	300*	ND	Pt–cure	Wearable	ND	44	18	2.44
Tang et al. (108)	Yes	Extrusion printing	1	350*	ND	PU	Wearable	ND	15	6	2.5
Reis Carneiro et al. (96)	Yes	DIW	1	200	ND	TPU	Wearable	ND	55	21	2.62
Valentine et al. (95)	Yes	Hybrid 3DP	1	100	ND	TPU	Wearable	ND	42	16	2.63
Tavakoli et al. (104)	Yes	Laser patterning	2	25	ND	Tegaderm	Wearable	ND	58	21	2.76[f]
Liu et al. (89)	Yes	Transfer printing	2	25	200	VHB	Wearable	ND	20	7	2.85
Yin et al. (109)	Yes	Selective wetting	1	ND	ND	PDMS	Robot	ND	72	24	3
Ozutemiz et al. (82)	Yes	Selective wetting	1	200*	40	PDMS	Wearable	ND	9	3	3
Lopes et al. (94)	Yes	DIW	1	200[g]	ND	SIS	Wearable	ND	47	15	3.13
Ozutemiz et al. (100)	Yes	Selective wetting	1	40	40	PDMS	NA	ND	29	9	3.22
Xie et al. (101)	Yes	Extrusion printing	2	ND	360	Pt–cure	Robot[h]	ND	25	6	4.16

(*Continued*)

Table 3 *(Continued)*

Reference	ICs?	Trace manufacturing technique	Num. layers[a]	Min. TW (μm)[b]	Max. strain (%)	Substrate	Application	Strain during application (%)	Num. rigid–soft interf.[c]	Num. rigid comp.[d]	Complexity num.[e]
Lopes et al. (98)	Yes	Extrusion printing	2	200	ND	SIS	Wearable	ND	35	8	4.38
Woodman et al. (102)	Yes	Screen printing	2	200	404	Pt.-cure and VHB	Robot	100	66	15	4.4
Hellebrekers et al. (97)	Yes	Selective wetting	1	200	ND	PDMS	Robot	ND	112	25	4.48
Zu et al. (110)	Yes	DIW	1	200	ND	Tegaderm	Wearable	ND	20	4	5

Note that because these numbers and the information from the rest of the table were derived only from the material available in the papers and supporting information, the information may be imperfect. However, if the numbers are not entirely correct, they are close, and they are reported here in an effort to summarize the trajectory of the field. Abbreviations: 3DP, 3D printing; DIW, direct ink write; IC, integrated circuit; NA, not applicable; ND, no data; PDMS, polydimethylsiloxane; Pt.-cure, platinum cure silicone (like those provided by SmoothOn Inc.); PU, polyurethane; SIS, styrene–isoprene–styrene block copolymer; TPU, thermoplastic urethane; TW, trace width; VHB, very-high-bond tape.

[a]Number of circuit layers.

[b]Minimum trace width reported or calculated for the process (not necessarily the complex circuit being analyzed in the rest of the table); values derived from figures rather than reported are marked with an asterisk.

[c]Number of rigid–soft interfaces, calculated by adding the number of times a rigid component (resistor, LED, integrated circuit, etc.) contacted a soft conductive trace; for example, a circuit with a single LED would have 2 interfaces, and a circuit with a 32-pin integrated circuit component with 10 traces connecting to 10 pads would have 10 interfaces (not 32).

[d]Number of rigid components, counted as the total number of integrated circuits, resistors, capacitors, diodes, and so on in the circuit; for example, a circuit with three resistors, one LED, and a microprocessor integrated circuit would have a total of five components.

[e]Complexity number (number of rigid–soft interfaces divided by number of rigid components).

[f]For blood oxygen level (SpO$_2$)–sensing circuit (highest complexity number).

[g]For extrusion printing method.

[h]The characterized circuit was not the one used in this application. The circuit used in the application had a complexity number of 3.9, and no strain data were reported.
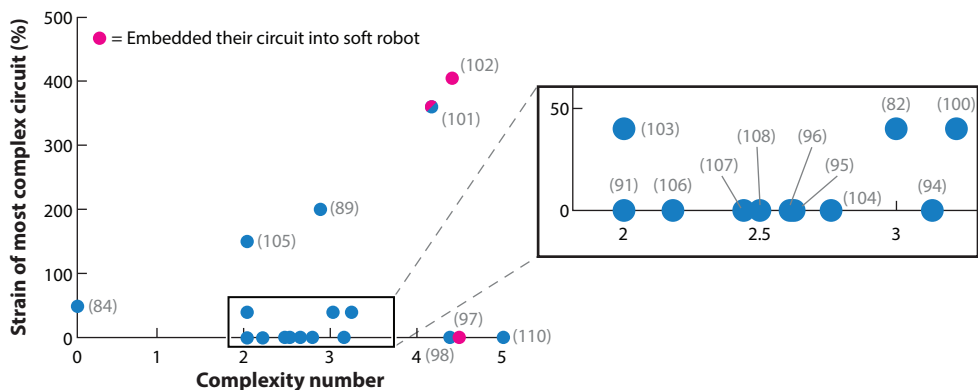
Figure 5

Plot of the maximum strain of the most complex circuit presented in several papers on stretchable electronics versus the complexity number (the number of rigid–soft interfaces divided by the number of rigid components in the circuit). If the circuit's performance during strain was not quantified or shown, we plotted it as zero. The number of rigid–soft interfaces was calculated by adding the number of times a rigid component (resistor, LED, integrated circuit, etc.) contacted a soft conductive trace; for example, a circuit with a single LED would have 2 interfaces, and a circuit with a 32-pin integrated circuit component with 10 traces connecting to 10 pads would have 10 interfaces (not 32). The number of microelectronic components is counted as the total number of integrated circuits, resistors, capacitors, diodes, and so on in the circuit; for example, a circuit with three resistors, one LED, and a microprocessor integrated circuit would have a total of five components. Note that because these numbers and the information from the rest of the table were derived only from the material available in the papers and supporting information, the information may be imperfect. However, if the numbers are not entirely correct, they are close, and they are reported here in an effort to summarize the trajectory of the field. Reference 101 is marked half pink and half blue because the circuit that was characterized (and plotted here) is not the one embedded in the robot.

platforms and their performance when embedded in soft, high-strain systems. This progression will lead to soft computation platforms that match the modulus of the application or robot, seamlessly integrate sensing, and move control onboard. These advancements, coupled with progress in stretchable, robot-agnostic shape sensing, will enable closed-loop control over shape in GSCRs, facilitating onboard control and moving us closer to realizing the vision of the field and the robotics community as a whole.

4. TOWARD CLOSED-LOOP SHAPE CONTROL

Having reviewed the current status of robot-agnostic shape sensing and stretchable computation, we now ask, How do these technologies synergize to achieve closed-loop shape control for future GSCRs?

Beginning with the sensing arrays (including stretch sensors and ICs for orientation sensing) summarized in **Table 2** and extending beyond the necessary improvements already discussed (to stretchability, level of integration into a shape-changing robot, and resolution), we note that the data from these sensors must be compiled and processed both locally and centrally to fulfill the objective of estimating a robot's shape. Onboard central computers should then be able to receive a desired shape and adjust the actuators accordingly to achieve this shape using the processed onboard shape-sensing data. Achieving the above functionality while retaining stretchability for morphing requires stretchable computation, as summarized in **Table 3**.

The techniques for implementing both robot-agnostic shape sensing and computation overlap. In **Table 2**, the solution with the highest level of compliance matching to a soft robotic

system, as well as the highest resolution of shape sensing, is achieved using techniques derived from the field of stretchable electronics. Combining the tools and methods from stretchable computation and robot-agnostic shape sensing propels us toward closed-loop shape control in soft robots.

Nevertheless, the algorithms needed to exploit this progress in materials and hardware must also be developed. The challenge of closing the loop on shape for shape-changing robots has not yet been thoroughly investigated. A few key initial methods have been put forth to accomplish inverse control of shape, which could be adapted in the future to robotic systems with onboard shape sensing. Wang et al. (111) used a deep learning algorithm, SMNet, to successfully demonstrate inverse control of 3D shape-morphing devices using point cloud data generated from simulations or offboard 3D scanners. In addition to using machine learning, which can be time and data intensive, methods in shape servoing could be relevant for closing the loop on shape. Shetab-Bushehri et al. (112) proposed lattice-based shape tracking and servoing of elastic objects that could successfully morph between known shapes. Such approaches could be adapted to realize closed-loop shape control in GSCRs using the materials and hardware reviewed herein.

5. CONCLUDING REMARKS

GSCRs hold the potential to realize the broad vision of robotics: machines capable of performing any task. Unrestricted by their morphology, GSCRs will leverage both biological and fantastical designs to efficiently accomplish various tasks. With advancements in robot-agnostic stretchable shape sensing and soft, stretchable computation, the initial examples of GSCRs with proprioception and closed-loop shape control are beginning to emerge.

In addition to sensing and computation, advancements in actuation (113), variable stiffness (114–116), structural materials (117), and control mechanisms (118, 119) are essential to fully realize GSCRs. Soft actuators should enable significant deformations, similar to pneumatic and hydraulic actuators, while allowing for untethered, independent motion, akin to electrically actuated devices such as dielectric elastomer (120) and piezoelectric actuators (121). GSCRs must also be capable of performing useful work. For instance, variable-stiffness limbs, like those introduced by Baines et al. (26), which soften to morph and stiffen to hold shape, highlight the necessity of such materials for effective shape morphing in GSCRs. Additionally, incorporating variable-stiffness materials, such as pressure-responsive, thermally responsive, and other types of materials, can enhance GSCR performance by using stiffness as a functional parameter.

Once the hardware for generic shape change is developed, several key questions arise. When and how should a robot decide to change shape? When is it energetically favorable? What are the most efficient methods for shape change? Overall, when is changing shape worth it? These are just the beginning of the intriguing and crucial questions we can explore with a platform capable of generalized shape change.

This review aimed to outline the state-of-the-art techniques for robot-agnostic shape sensing and stretchable computation. We hope it serves as a valuable resource for the development of GSCRs that can efficiently adapt their morphology and behavioral control policies to meet diverse tasks and environmental challenges.

SUMMARY POINTS

1. A significant gap exists between today's shape-changing robots and the envisioned general shape-changing robots (GSCRs).

2. Robot-agnostic stretchable shape sensing and stretchable computation are crucial components that will enable closed-loop control for future GSCRs.

3. Advancements in stretchable electronics and interfacial science are likely to mature current examples of soft, stretchable shape sensing and onboard computation.

FUTURE ISSUES

1. Addressing the key challenges we outlined in this work will be pivotal for achieving closed-loop shape control in soft robots, marking a significant step forward for the field.

2. Improving the stretchability and resolution of shape-sensing arrays is necessary to capture dynamic and complex shapes.

3. Advancements in interfacing between soft and rigid materials (e.g., soft traces and rigid integrated circuits) are essential for the successful implementation of stretchable electronics in general shape-changing robots.

DISCLOSURE STATEMENT

S.J.W. and R.K.-B. are listed as inventors on US continuation-in-part application 18/148,500, which claims priority to US patent application 17/357,060, on which R.K.-B. is also an inventor. This patent application protects stretchable circuit technology that is related to the content reviewed here.

ACKNOWLEDGMENTS

LITERATURE CITED

1. Shah D, Yang B, Kriegman S, Levin M, Bongard J, Kramer-Bottiglio R. 2021. Shape changing robots: bioinspiration, simulation, and physical realization. *Adv. Mater.* 33(19):2002882

2. Seo J, Paik J, Yim M. 2019. Modular reconfigurable robotics. *Annu. Rev. Control Robot. Auton. Syst.* 2:63–88

3. Belke CH, Holdcroft K, Sigrist A, Paik J. 2023. Morphological flexibility in robotic systems through physical polygon meshing. *Nat. Mach. Intell.* 5(6):669–75

4. Modes CD, Bhattacharya K, Warner M. 2011. Gaussian curvature from flat elastica sheets. *Proc. R. Soc. A* 467(2128):1121–40

5. Shepherd RF, Ilievski F, Choi W, Morin SA, Stokes AA, et al. 2011. Multigait soft robot. *PNAS* 108(51):20400–403

6. Tolley MT, Shepherd RF, Mosadegh B, Galloway KC, Wehner M, et al. 2014. A resilient, untethered soft robot. *Soft Robot.* 1(3):213–23

7. Rus D, Tolley MT. 2015. Design, fabrication and control of soft robots. *Nature* 521(7553):467–75

8. Rich SI, Wood RJ, Majidi C. 2018. Untethered soft robotics. *Nat. Electron.* 1(2):102–12

9. Shah DS, Powers JP, Tilton LG, Kriegman S, Bongard J, Kramer-Bottiglio R. 2021. A soft robot that adapts to environments through shape change. *Nat. Mach. Intell.* 3(1):51–59. Correction. 2024. *Nat. Mach. Intell.* 6(4):493

10. Baines R, Fish F, Bongard J, Kramer-Bottiglio R. 2024. Robots that evolve on demand. *Nat. Rev. Mater.* 9(11):822–35

11. Wharton P, You TL, Jenkinson GP, Diteesawat RS, Le NH, et al. 2023. Tetraflex: a multigait soft robot for object transportation in confined environments. *IEEE Robot. Autom. Lett.* 8(8):5007–14

12. Steltz E, Mozeika A, Rodenberg N, Brown E, Jaeger HM. 2009. JSEL: jamming skin enabled locomotion. In *2009 IEEE/RSJ International Conference on Intelligent Robots and Systems*, pp. 5672–77. Piscataway, NJ: IEEE

13. Kim T, Lee S, Chang S, Hwang S, Park YL. 2023. Environmental adaptability of legged robots with cutaneous inflation and sensation. *Adv. Intell. Syst.* 5(11):2300172

14. Zhakypov Z, Mori K, Hosoda K, Paik J. 2019. Designing minimal and scalable insect-inspired multilocomotion millirobots. *Nature* 571(7765):381–86

15. McEvoy MA, Correll N. 2018. Shape-changing materials using variable stiffness and distributed control. *Soft Robot.* 5(6):737–47

16. Stella F, Santina CD, Hughes J. 2023. Soft robot shape estimation with IMUs leveraging PCC kinematics for drift filtering. *IEEE Robot. Autom. Lett.* 9(2):1945–52

17. Yang X, Zhou Y, Zhao H, Huang W, Wang Y, et al. 2023. Morphing matter: from mechanical principles to robotic applications. *Soft Sci.* 3(4):38

18. Pikul JH, Li S, Bai H, Hanlon RT, Cohen I, Shepherd RF. 2017. Stretchable surfaces with programmable 3D texture morphing for synthetic camouflaging skins. *Science* 358(6360):210–14

19. Siéfert E, Reyssat E, Bico J, Roman B. 2018. Bio-inspired pneumatic shape-morphing elastomers. *Nat. Mater.* 18(1):24–28

20. Devlin MR, Liu T, Zhu M, Usevitch NS, Colonnese N, Memar AH. 2023. Soft, modular, shape-changing displays with hyperelastic bubble arrays. In *2023 IEEE/RSJ International Conference on Intelligent Robots and Systems*, pp. 5101–6. Piscataway, NJ: IEEE

21. Hanuhov T, Cohen N. 2023. Design principles for 3D-printed thermally activated shape-morphing structures. *Int. J. Mech. Sci.* 262:108716

22. Zhang K, Zhou Y, Zhang J, Liu Q, Hanenberg C, et al. 2024. Shape morphing of hydrogels by harnessing enzyme enabled mechanoresponse. *Nat. Commun.* 15(1):249

23. Johnson K, Arroyos V, Ferran A, Villanueva R, Yin D, et al. 2023. Solar-powered shape-changing origami microfliers. *Sci. Robot.* 8(82):eadg4276

24. Lin HT, Leisk GG, Trimmer B. 2011. GoQBot: a caterpillar-inspired soft-bodied rolling robot. *Bioinspir. Biomim.* 6(2):026007

25. Sun J, Lerner E, Tighe B, Middlemist C, Zhao J. 2023. Embedded shape morphing for morphologically adaptive robots. *Nat. Commun.* 14(1):6023

26. Baines R, Patiballa SK, Booth J, Ramirez L, Sipple T, et al. 2022. Multi-environment robotic transitions through adaptive morphogenesis. *Nature* 610(7931):283–89

27. Shah DS, Yuen MC, Tilton LG, Yang EJ, Kramer-Bottiglio R. 2019. Morphing robots using robotic skins that sculpt clay. *IEEE Robot. Autom. Lett.* 4(2):2204–11

28. Sun J, Zhao J. 2019. An adaptive walking robot with reconfigurable mechanisms using shape morphing joints. *IEEE Robot. Autom. Lett.* 4(2):724–31

29. Nygaard TF, Martin CP, Torresen J, Glette K, Howard D. 2021. Real-world embodied AI through a morphologically adaptive quadruped robot. *Nat. Mach. Intell.* 3(5):410–19

30. Jeong J, Kim I, Choi Y, Lim S, Kim S, et al. 2023. Spikebot: a multigait tensegrity robot with linearly extending struts. *Soft Robot.* 11(2):207–17

31. Hwang D, Barron EJ, Tahidul Haque AB, Bartlett MD. 2022. Shape morphing mechanical metamaterials through reversible plasticity. *Sci. Robot.* 7(63):2171

32. Wilcox BT, Joyce J, Bartlett MD. 2024. Rapid and reversible morphing to enable multifunctionality in robots. *Adv. Intell. Syst.* **https://doi.org/10.1002/aisy.202300694**

33. Lee DY, Kim SR, Kim JS, Park JJ, Cho KJ. 2017. Origami wheel transformer: a variable-diameter wheel drive robot using an origami structure. *Soft Robot.* 4(2):163–80

34. Yoon H, Kim SG, Park I, Heo J, Kim HS, Seo TW. 2024. 2 DOF transformable wheel design based on geared 8 bar parallel linkage mechanism. *Sci. Rep.* 14(1):379

35. Baines R, Freeman S, Fish F, Kramer-Bottiglio R. 2020. Variable stiffness morphing limb for amphibious legged robots inspired by chelonian environmental adaptations. *Bioinspir. Biomim.* 15(2):025002

36. White EL, Yuen MC, Case JC, Kramer RK. 2017. Low-cost, facile, and scalable manufacturing of capacitive sensors for soft systems. *Adv. Mater. Technol.* 2(9):1700072

37. Johnson WR, Agrawala A, Huang X, Booth J, Kramer-Bottiglio R. 2022. Sensor tendons for soft robot shape estimation. In *2022 IEEE Sensors*. Piscataway, NJ: IEEE. **https://doi.org/10.1109/SENSORS52175.2022.9967136**

38. Sanchez-Botero L, Agrawala A, Kramer-Bottiglio R. 2023. Stretchable, breathable, and washable fabric sensor for human motion monitoring. *Adv. Mater. Technol.* 8(17):2300378

39. Shih B, Shah D, Li J, Thuruthel TG, Park YL, et al. 2020. Electronic skins and machine learning for intelligent soft robots. *Sci. Robot.* 5(41):9239

40. Thuruthel TG, Shih B, Laschi C, Tolley MT. 2019. Soft robot perception using embedded soft sensors and recurrent neural networks. *Sci. Robot.* 4(26):1488

41. Baines R, Zuliani F, Chennoufi N, Joshi S, Kramer-Bottiglio R, Paik J. 2023. Multi-modal deformation and temperature sensing for context-sensitive machines. *Nat. Commun.* 14(1):7499

42. Chen F, Song Z, Chen S, Gu G, Zhu X. 2023. Morphological design for pneumatic soft actuators and robots with desired deformation behavior. *IEEE Trans. Robot.* 39(6):4408–28

43. Mengaldo G, Renda F, Brunton SL, Bächer M, Calisti M, et al. 2022. A concise guide to modelling the physics of embodied intelligence in soft robotics. *Nat. Rev. Phys.* 4(9):595–610

44. Tairych A, Anderson IA. 2019. Capacitive stretch sensing for robotic skins. *Soft Robot.* 6(3):389–98

45. Shintake J, Piskarev E, Jeong SH, Floreano D. 2018. Ultrastretchable strain sensors using carbon black-filled elastomer composites and comparison of capacitive versus resistive sensors. *Adv. Mater. Technol.* 3(3):1700284

46. Tapia J, Knoop E, Mutný M, Otaduy MA, Bächer M. 2020. MakeSense: automated sensor design for proprioceptive soft robots. *Soft Robot.* 7(3):332–45

47. Li L, Xue M, Xu T, Liu Y, Yuan Y, Lin Z. 2023. Intelligent soft self-twisted shape sensor. *Phys. Lett. A* 492:129219

48. Galloway KC, Chen Y, Templeton E, Rife B, Godage IS, Barth EJ. 2019. Fiber optic shape sensing for soft robotics. *Soft Robot.* 6(5):671–84

49. Wang F, Jiang Q, Li J. 2023. Shape sensing for continuum robots using FBG sensors array considering bending and twisting. *IEEE Sens. J.* 24(2):1546–54

50. Van Meerbeek IM, De Sa CM, Shepherd RF. 2018. Soft optoelectronic sensory foams with proprioception. *Sci. Robot.* 3(24):eaau248

51. Ju H, Cha B, Rus D, Lee J. 2023. Closed-loop soft robot control frameworks with coordinated policies based on reinforcement learning and proprioceptive self-sensing. *Adv. Funct. Mater.* 33(51):2304642

52. McEvoy MA, Correll N. 2015. Materials that couple sensing, actuation, computation, and communication. *Science* 347(6228):1261689

53. Hoshi T, Shinoda H. 2008. 3D shape measuring sheet utilizing gravitational and geomagnetic fields. In *2008 SICE Annual Conference*, pp. 915–20. Madrid: SICE

54. Hermanis A, Cacurs R, Greitans M. 2016. Acceleration and magnetic sensor network for shape sensing. *IEEE Sens. J.* 16(5):1271–80

55. Zhou Z, Chen P, Lu Y, Cui Q, Pan D, et al. 2023. 3D deformation capture via a configurable self-sensing IMU sensor network. *Proc. ACM Interact. Mob. Wearable Ubiquitous Technol.* 7(1):42

56. Stanko T, Hahmann S, Bonneau GP, Saguin-Sprynski N. 2017. Shape from sensors: curve networks on surfaces from 3D orientations. *Comput. Graph.* 66:74–84

57. Shah D, Woodman SJ, Sanchez-Botero L, Liu S, Kramer-Bottiglio R. 2023. Stretchable shape-sensing sheets. *Adv. Intell. Syst.* 5(12):2300343

58. Sprynski N, Szafran N, Lacolle B, Biard L. 2008. Surface reconstruction via geodesic interpolation. *Comput.-Aided Des.* 40(4):480–92

59. Huard M, Sprynski N, Szafran N, Biard L. 2013. Reconstruction of quasi developable surfaces from ribbon curves. *Numer. Algorithms* 63(3):483–506

60. Huard M, Farouki RT, Sprynski N, Biard L. 2014. C2 interpolation of spatial data subject to arc-length constraints using Pythagorean–hodograph quintic splines. *Graph. Models* 76(1):30–42

61. Saguin-Sprynski N, Jouanet L, Lacolle B, Biard L. 2014. Surfaces reconstruction via inertial sensors for monitoring. *e-J. Nondestr. Test.* 20(2):702–9

62. Hu Y, Yan Y, Efstratiou C, Vela-Orte D. 2021. Quantitative shape measurement of an inflatable rubber dam using an array of inertial measurement units. *IEEE Trans. Instrum. Meas.* 70:9506310

63. Rendl C, Kim D, Fanello S, Parzer P, Rhemann C, et al. 2014. FlexSense: a transparent self-sensing deformable surface. In *UIST '14: Proceedings of the 27th Annual ACM Symposium on User Interface Software and Technology*, pp. 129–38. New York: ACM

64. Mittendorfer P, Dean E, Cheng G. 2014. 3D spatial self-organization of a modular artificial skin. In *2014 IEEE/RSJ International Conference on Intelligent Robots and Systems*, pp. 3969–74. Piscataway, NJ: IEEE

65. Woodman SJ, Agrawala A, Kramer-Bottiglio R. 2023. Stretchable shape-sensing ribbons. In *2023 IEEE SENSORS*. Piscataway, NJ: IEEE. **https://doi.org/10.1109/SENSORS56945.2023.10325035**

66. Lun TLT, Wang K, Ho JD, Lee KH, Sze KY, Kwok KW. 2019. Real-time surface shape sensing for soft and flexible structures using fiber Bragg gratings. *IEEE Robot. Autom. Lett.* 4(2):1454–61

67. Soleimani M, Dingley G, Semaj E, Petrou M. 2023. Shape self-sensing with mutual inductance sensor array. *IEEE Sens. J.* 23(20):25234–41

68. Ledezma FD, Haddadin S. 2023. Machine learning–driven self-discovery of the robot body morphology. *Sci. Robot.* 8(85):972

69. Shannon CE. 1949. Communication in the presence of noise. *Proc. IRE* 37(1):10–21

70. Stokes AA, Shepherd RF, Morin SA, Ilievski F, Whitesides GM. 2014. A hybrid combining hard and soft robots. *Soft Robot.* 1(1):70–74

71. Hao T, Xiao H, Ji M, Liu Y, Liu S. 2023. Integrated and intelligent soft robots. *IEEE Access* 11:99862–77

72. Preston DJ, Rothemund P, Jiang HJ, Nemitz MP, Rawson J, et al. 2019. Digital logic for soft devices. *PNAS* 116(16):7750–59

73. Rothemund P, Ainla A, Belding L, Preston DJ, Kurihara S, et al. 2018. A soft, bistable valve for autonomous control of soft actuators. *Sci. Robot.* 3(16):eaar7986

74. Conrad S, Teichmann J, Auth P, Knorr N, Ulrich K, et al. 2024. 3D-printed digital pneumatic logic for the control of soft robotic actuators. *Sci. Robot.* 9(86):eadh4060

75. Drotman D, Jadhav S, Sharp D, Chan C, Tolley MT. 2021. Electronics-free pneumatic circuits for controlling soft-legged robots. *Sci. Robot.* 6(51):2627

76. Toepke MW, Abhyankar VV, Beebe DJ. 2007. Microfluidic logic gates and timers. *Lab Chip* 7(11):1449–53

77. Prakash M, Gershenfeld N. 2007. Microfluidic bubble logic. *Science* 315(5813):832–35

78. El Helou C, Buskohl PR, Tabor CE, Harne RL. 2021. Digital logic gates in soft, conductive mechanical metamaterials. *Nat. Commun.* 12(1):1633

79. Rogers JA, Someya T, Huang Y. 2010. Materials and mechanics for stretchable electronics. *Science* 327(5973):1603–7

80. Reis Carneiro M, Majidi C, Tavakoli M. 2023. Gallium-based liquid–solid biphasic conductors for soft electronics. *Adv. Funct. Mater.* 33(41):2306453

81. Dickey MD. 2017. Stretchable and soft electronics using liquid metals. *Adv. Mater.* 29(27):1606425

82. Ozutemiz KB, Majidi C, Ozdoganlar OB. 2022. Scalable manufacturing of liquid metal circuits. *Adv. Mater. Technol.* 7(11):2200295

83. Bai H, Hu Z, Rogers JA. 2023. Hybrid materials approaches for bioelectronics. *MRS Bull.* 48(11):1125–39

84. Huang Z, Hao Y, Li Y, Hu H, Wang C, et al. 2018. Three-dimensional integrated stretchable electronics. *Nat. Electron.* 1(8):473–80

85. Liu ZF, Fang S, Moura FA, Ding JN, Jiang N, et al. 2015. Hierarchically buckled sheath-core fibers for superelastic electronics, sensors, and muscles. *Science* 349(6246):400–4

86. Eristoff S, Nasab AM, Huang X, Kramer-Bottiglio R. 2023. Liquid metal + x: a review of multiphase composites containing liquid metal and other (x) fillers. *Adv. Funct. Mater.* 34(31):2309529

87. Kazem N, Hellebrekers T, Majidi C. 2017. Soft multifunctional composites and emulsions with liquid metals. *Adv. Mater.* 29(27):1605985

88. Daalkhaijav U, Yirmibesoglu OD, Walker S, Mengüç Y. 2018. Rheological modification of liquid metal for additive manufacturing of stretchable electronics. *Adv. Mater. Technol.* 3(4):1700351

89. Liu S, Shah DS, Kramer-Bottiglio R. 2021. Highly stretchable multilayer electronic circuits using biphasic gallium-indium. *Nat. Mater.* 20(6):851–58

90. Sanchez-Botero L, Shah DS, Kramer-Bottiglio R. 2022. Are liquid metals bulk conductors? *Adv. Mater.* 34(26):2109427

91. Chen S, Fan S, Qi J, Xiong Z, Qiao Z, et al. 2023. Ultrahigh strain-insensitive integrated hybrid electronics using highly stretchable bilayer liquid metal based conductor. *Adv. Mater.* 35(5):2208569

92. Pan C, Kumar K, Li J, Markvicka EJ, Herman PR, et al. 2018. Visually imperceptible liquid-metal circuits for transparent, stretchable electronics with direct laser writing. *Adv. Mater.* 30(12):1706937

93. Zrnic D, Swatik DS. 1969. On the resistivity and surface tension of the eutectic alloy of gallium and indium. *J. Less Common Met.* 18(1):67–68

94. Lopes PA, Santos BC, de Almeida AT, Tavakoli M. 2021. Reversible polymer-gel transition for ultra-stretchable chip-integrated circuits through self-soldering and self-coating and self-healing. *Nat. Commun.* 12(1):4666

95. Valentine AD, Busbee TA, Boley JW, Raney JR, Chortos A, et al. 2017. Hybrid 3D printing of soft electronics. *Adv. Mater.* 29(40):1703817

96. Reis Carneiro M, de Almeida AT, Tavakoli M, Majidi C. 2023. Recyclable thin-film soft electronics for smart packaging and e-skins. *Adv. Sci.* 10(26):2301673

97. Hellebrekers T, Ozutemiz KB, Yin J, Majidi C. 2018. Liquid metal-microelectronics integration for a sensorized soft robot skin. In *2018 IEEE/RSJ International Conference on Intelligent Robots and Systems*, pp. 5924–29. Piscataway, NJ: IEEE

98. Lopes PA, Fernandes DF, Silva AF, Marques DG, De Almeida AT, et al. 2021. Bi-phasic Ag–In–Ga-embedded elastomer inks for digitally printed, ultra-stretchable, multi-layer electronics. *ACS Appl. Mater. Interfaces* 13(12):14552–61

99. Kim S, Yoo D, Lim J, Kim J. 2024. Simple and effective patterning method of liquid-metal-infused sponge electrode for fabricating 3D stretchable electronics. *Adv. Mater. Technol.* 9(14):2301589

100. Ozutemiz KB, Wissman J, Ozdoganlar OB, Majidi C. 2018. EGaIn–metal interfacing for liquid metal circuitry and microelectronics integration. *Adv. Mater. Interfaces* 5(10):1701596

101. Xie Z, Yuan F, Liu J, Tian L, Chen B, et al. 2023. Octopus-inspired sensorized soft arm for environmental interaction. *Sci. Robot.* 8(84):eadh7582

102. Woodman SJ, Shah DS, Landesberg M, Agrawala A, Kramer-Bottiglio R. 2024. Stretchable Arduinos embedded in soft robots. *Sci. Robot.* 9(94):eadn6844

103. Lee B, Cho H, Moon S, Ko Y, Ryu YS, et al. 2023. Omnidirectional printing of elastic conductors for three-dimensional stretchable electronics. *Nat. Electron* 6(4):307–18

104. Tavakoli M, Lopes PA, Hajalilou A, Silva AF, Reis Carneiro M, et al. 2022. 3R electronics: scalable fabrication of resilient, repairable, and recyclable soft-matter electronics. *Adv. Mater.* 34(31):2203266

105. Song S, Hong H, Kim KY, Kim KK, Kim J, et al. 2023. Photothermal lithography for realizing a stretchable multilayer electronic circuit using a laser. *ACS Nano* 17(21):21443–54

106. Lee DH, Lim T, Pyeon J, Park H, Lee SW, et al. 2024. Self-mixed biphasic liquid metal composite with ultra-high stretchability and strain-insensitivity for neuromorphic circuits. *Adv. Mater.* 36(16):2310956

107. Li G, Zhang M, Liu S, Yuan M, Wu J, et al. 2023. Three-dimensional flexible electronics using solidified liquid metal with regulated plasticity. *Nat. Electron.* 6(2):154–63

108. Tang L, Yang S, Zhang K, Jiang X, Tang L, et al. 2022. Skin electronics from biocompatible in situ welding enabled by intrinsically sticky conductors. *Adv. Sci.* 9(23):2202043

109. Yin J, Hellebrekers T, Majidi C. 2020. Closing the loop with liquid-metal sensing skin for autonomous soft robot gripping. In *2020 3rd IEEE International Conference on Soft Robotics*, pp. 661–67. Piscataway, NJ: IEEE

110. Zu W, Ohm Y, Carneiro MR, Vinciguerra M, Tavakoli M, Majidi C. 2022. A comparative study of silver microflakes in digitally printable liquid metal embedded elastomer inks for stretchable electronics. *Adv. Mater. Technol.* 7(12):2200534

111. Wang J, Sarkar D, Suo J, Chortos A. 2024. Harnessing deep learning of point clouds for inverse control of 3D shape morphing. arXiv:2401.15219 [cs.RO]

112. Shetab-Bushehri M, Aranda M, Mezouar Y, Ozgur E. 2024. Lattice-based shape tracking and servoing of elastic objects. *IEEE Trans. Robot.* 40:364–81

113. Li M, Pal A, Aghakhani A, Pena-Francesch A, Sitti M. 2021. Soft actuators for real-world applications. *Nat. Rev. Mater.* 7(3):235–49

114. Manti M, Cacucciolo V, Cianchetti M. 2016. Stiffening in soft robotics: a review of the state of the art. *IEEE Robot. Autom. Mag.* 23(3):93–106

115. Gao M, Meng Y, Shen C, Pei Q. 2022. Stiffness variable polymers comprising phase-changing side-chains: material syntheses and application explorations. *Adv. Mater.* 34(21):2109798

116. Levine DJ, Turner KT, Pikul JH. 2021. Materials with electroprogrammable stiffness. *Adv. Mater.* 33(35):2007952

117. Chi Y, Li Y, Zhao Y, Hong Y, Tang Y, et al. 2022. Bistable and multistable actuators for soft robots: structures, materials, and functionalities. *Adv. Mater.* 34(19):2110384

118. Della Santina C, Duriez C, Rus D. 2023. Model-based control of soft robots: a survey of the state of the art and open challenges. *IEEE Control Syst.* 43(3):30–65

119. Wang J, Chortos A. 2022. Control strategies for soft robot systems. *Adv. Intell. Syst.* 4(5):2100165

120. Guo Y, Liu L, Liu Y, Leng J. 2021. Review of dielectric elastomer actuators and their applications in soft robots. *Adv. Intell. Syst.* 3(10):2000282

121. El-Atab N, Mishra RB, Al-Modaf F, Joharji L, Alsharif AA, et al. 2020. Soft actuators for soft robotic applications: a review. *Adv. Intell. Syst.* 2(10):2000128